GEO-FPN: A convolutional neural network for detecting GEO and near-GEO space objects from optical images

Rasit Abay[(1)] and Komal Gupta[(1)]

[(1)]FuturifAI, Australian Capital Territory, Australia, {r.abay, komal.gupta}@futurifai.com

ABSTRACT

Surveillance of resident space objects (RSOs) is essential for detection, tracking, and cataloguing them to keep active satellites safe from hazards. High altitude space objects are observed using optical telescopes due to their efficiency. However, it is labour-intensive to detect space objects in the images captured by telescopes, and automation is desired. The proposed framework leverages the Feature Pyramid Network (FPN), a convolutional neural network for image segmentation, to automate RSO detection in the telescope images. The backbone used for detecting low-level patterns from images is the pre-trained EfficientNet-B7 on ImageNet. A simple preprocessing is applied to images that are overexposed to scale the input image pixel values, and this thresholding is only conducted using the statistics of the training data. A custom deterministic post-processing method based on vector mathematics is developed to clean the false detections. F1 score of the proposed machine learning framework is 92%, and this performance shows that the convolutional neural networks can be utilised for automating RSO detection from telescope images.

1 INTRODUCTION

Satellites are an integral part of modern society, and many industries depend on them to function every day. It is essential to detect, track, and catalog resident space objects for keeping operational satellites safe from probable collisions. Space Domain Awareness (SDA) is concerned with detecting threats to operational satellites by utilising space surveillance sensors [1]. Due to the improved SDA sensors and the accessibility of cheaper electronics, the number of trackable objects is increasing, and some level of automation is essential to keep pace with the number of resident space objects (RSOs) [2,5]. The most widely used sensor types for space surveillance are optical telescopes and radars. Due to the efficiency of the optical sensors for higher altitudes, RSOs in geostationary (GEO) and near-geostationary (near-GEO) orbits are observed with the optical telescopes [3, 4]. The automation in detecting the space objects in the optical images can decrease the manpower needed for the task, and reduce the false detections.

In the literature, there are two different approaches to detect space objects from optical telescope images, namely stacking methods and line-fitting methods. The stacking methods enable detecting faint objects by stacking multiple images together and using filters such as median filter [6,7,8]. Although the stacking method is effective in detecting faint signals in the images, its downside is the time required to conduct analysis for an object whose movement is not known, and its implementation on accelerated hardware is required [8]. Line-fitting methods search for possible tracks to determine the space objects in the sequences of images [8, 9, 10]. They are suitable for online data processing, and they do not require the speed and the motion direction of space objects detected. However, it is not always possible to detect faint objects in a single image [10]. Recently, the application of data-driven approaches for the optical detection of GEO objects has attracted attention [11]. Gaussian process regression (GPR) with line-fitting and topological sweep have shown promising results in detecting faint objects in the telescope images [11,12]. GPR has been developed for removing the background in the images [11,12], and it can adapt to data better than hand-crafted methods [10]. However, it is desired to develop learning-based algorithms that directly learn from data, and can be trained end-to-end to reduce the false detections.

Proc. 8th European Conference on Space Debris (virtual), Darmstadt, Germany, 20–23 April 2021, published by the ESA Space Debris Office
Ed. T. Flohrer, S. Lemmens & F. Schmitz, (http://conference.sdo.esoc.esa.int, May 2021)

Therefore, this research investigates the feasibility of using machine learning, namely convolutional neural networks, to detect RSOs by training end-to-end on low-cost telescope images.

The outline of the rest of the proposed work is : Section 2 introduces the data and the data preprocessing processes used to prepare data for the proposed machine learning framework. Section 3 explains the proposed convolutional neural network framework to segment space objects in the images and the proposed post-processing method that conducts multi-model fitting of objects detected in the sequences of frames. Section 4 presents the performance of the proposed solution and hard samples that challenge it. Section 5 provides conclusion and future work.

2 DATA

In 2020, ESA and University of Adelaide organised a challenge that invited experts around the World to develop computer vision algorithms for detecting faint space objects in the low-cost telescope images [13]. The proposed problem is detecting GEO and near-GEO satellites in the sequences of 5 frames without any associated orbital information regarding the space objects in the frames. The images are taken by a low-cost telescope located in Adelaide and saved in the PNG format. All objects are captured in all 5 frames. The camera is kept fixed for 40 seconds exposure time, and a fixed angle is used for tracking the space objects for each event. There are 1280 grayscale image sequences in the training dataset. The main challenge associated with the problem is the distance between the telescope and the space objects at high altitudes (35000-36000 km), and this leads to faint signals of the objects that are sometimes smeared in a couple of pixels in the image. In addition, atmospheric/weather conditions, light pollution, sensor noise/defects, and star occlusion are factors that make foreground and background segmentation a challenging task.

Training data is split using a stratified 5-fold cross-validation approach based on the number of objects in the images. Each image is renamed using image hashing, and a new data frame is generated that includes image names, sequence id, frame number, and the details regarding the split. Note that an additional algorithm based on image hashing verifies that no image that has a very similar distribution ends up in the same split to avoid probable data leakage. The image similarity step is added due to the fact that there is one ground location that the images are taken, and it can conduct surveillance of some specific region of the geostationary orbit regime. The histogram of the mean of pixel values for training images indicates that the number of overexposed images is relatively small (Figure 1). Therefore, the mean of pixel values of training images without including validation or test data are computed, and they are used to scale the overexposed images.

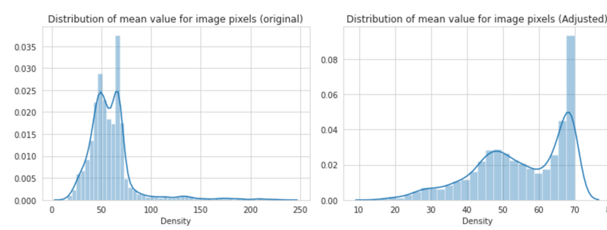

Figure 1. The distribution of mean pixel values of training images (left: original distribution and right: adjusted distribution).

The labels for space objects are indifferent to the fact that some labels have no corresponding signal in the image due to cloud cover, atmospheric/weather effects, light pollution, sensor noise/defects, and star occlusions. Since the proposed approach is a data-driven model, such noisy labels should be addressed. However, this requires some manual effort to do robust label denoising. Instead, the authors leveraged a mask generation approach that takes the point in a bounding box of size 4 by 4, and normalises pixel values within the bounding box and thresholds with 0.5, finally dilutes the point with a kernel of 1 and uses 2 by 2 window only. This approach is intended to generate a mask for the region of interest that is noticeable within the object's close vicinity (Figure 2).

Figure 2. The mask generated for an object of interest using the proposed masking approach (left: object mask and right: object image).

3 METHODOLOGY

3.1 Feature Pyramid Network (FPN) for Object Detection

Feature Pyramid Network (FPN) is a feature extractor that can be leveraged for image segmentation and object detection. It converts a single image to feature maps that are proportionally sized at different levels. Data flows in two different directions, namely bottom-up and top-down. In the bottom-top pathway, resolution decreases and feature value for each layer increases (Figure 3). In addition, the bottom-top part can utilise feature extractors such as EfficientNet [15]. The proposed FPN uses EfficientNet-B7 that is pre-trained on ImageNet dataset. In the top-down pathway, feature value for each layer decreases and resolution increases. For better spatial awareness of the feature maps, FPN leverages lateral skip connections [14].

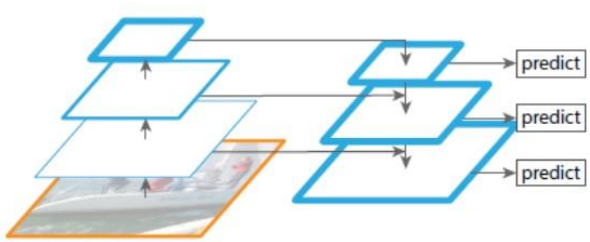

Figure 3. The visual representation of Feature Pyramid Networks.

The loss function utilised is dice loss for the proposed framework. Dice loss is a region-based loss, and it intends to maximize the overlapping between the ground truth and predicted segmentation. The metric for training is intersection over union (IOU) with a threshold of 0.5. Learning rate is 0.0001, and the optimizer is Adam for faster convergence. Batch size is 2 and the number of training epochs is 100 for each fold. Majority vote is used to ensemble the predictions. The hardware used for training is two NVIDIA RTX 2080 Ti.

$$Dice\ Loss = 1 - \frac{2|G \cap S|}{|G| + |S|}. \tag{1}$$

3.2 Post-Processing for the Predictions of the Proposed Model

Some objects can not be detected in frames due to cloud cover, atmospheric/weather effects, light pollution, sensor noise/defects, and star occlusions. Since space objects in the images are captured in all 5 frames, it is possible to conduct multi-model fitting for masks generated by FPN. Due to the nature of GEO and near-GEO orbits, fitting a line on the detected masks reveals objects in the image sequences. In addition, the movement of objects in the images are perpendicularly constrained and the distance between each mask detected for the same object should be equally spaced in subsequent frames (Note that the movement of camera between exposures is kept fixed for each event). A visual representation of the proposed post-processing method is presented in Figure 4.

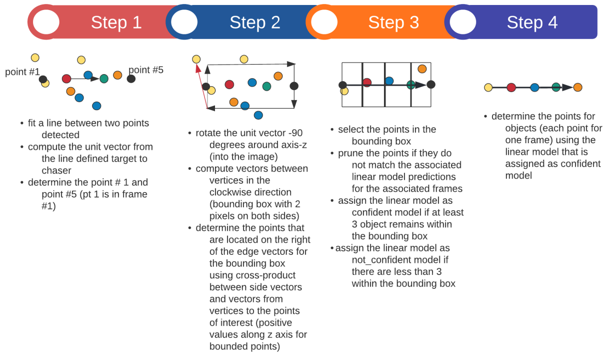

Figure 4. The proposed post-processing method based on vector mathematics.

4 RESULTS

4.1 Performance of GEO-FPN for RSO Detection

The proposed GEO-FPN model detects RSOs by generating masks for them. The following images show the visual performance of our model (Figure 5). The ground truth masks denote the true location of the objects in the input image, while the predicted masks are the outputs of the model.

It is evident from the examples in Figure 5 that the proposed model is capable of detecting very faint objects in images impacted by noise, and some of which are difficult to see through human eyes. In addition, the model also detects objects that appear very close to each other. Overall, the F1 score of the GEO-FPN model is 88% in detecting RSOs in the images. Further improvement is achieved by using a custom post-processing algorithm, which is described in the following section.

Figure 5a

Figure 5b

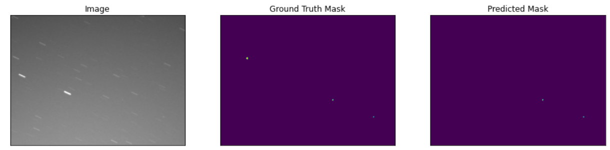

Figure 5c

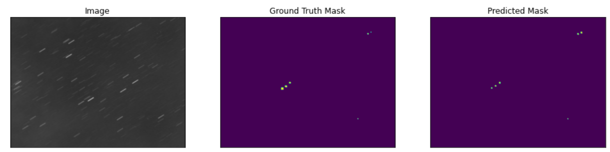

Figure 5. Results of GEO-FPN model: (a) for extremely faint objects (b) for noisy input image (c) for crowded scenes

4.2 Improvement in Predictions using Post-Processing

In Fig 5(b), it can be seen that the model misses one of the objects in the image, likely due to overexposure of the image. Moreover, atmospheric effects and other noise cause the model to miss some faint objects, and make false predictions. We deal with these cases by using our post-processing algorithm which cleans false detections as well as recovers the missed objects. The results after post-processing are shown below. The plots show the RSOs as it moves through the sequence of frames by stacking the outputs of the model for each frame in the sequence. "+" symbols mark the true locations of objects in each frame, coloured circles denote the predicted locations of the objects in each of the five frames, and "×" symbols mark the predicted locations of the objects after post-processing has been applied.

Figure 6a

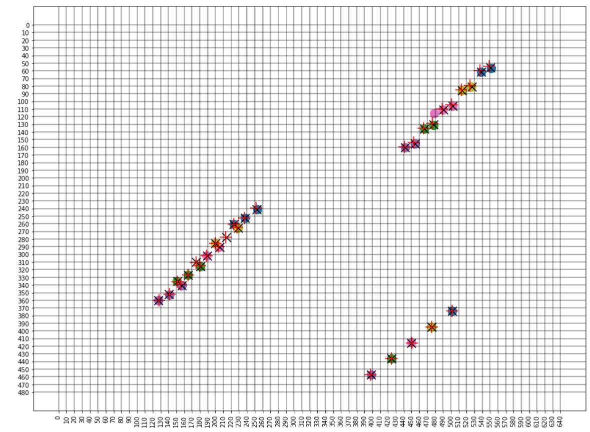

Figure 6b

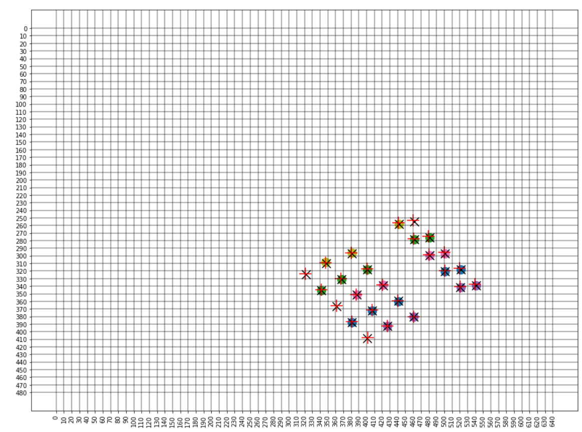

Figure 6c

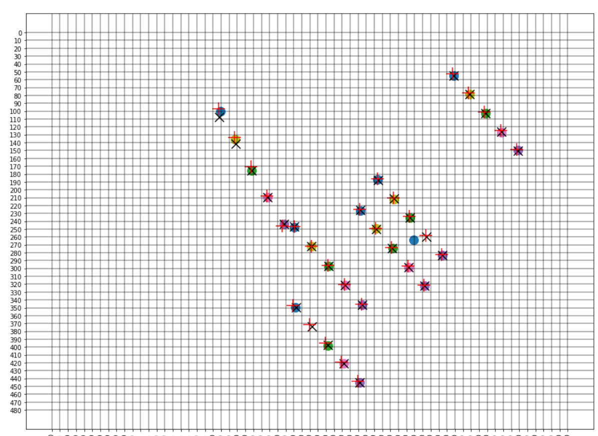

Figure 6: Final results of ML framework in the presence of crowded scenes with both false positives and missed detections (false negatives)

The post-processing boosts the F1 score of the proposed model to 92%, which is a significant improvement (4%) over the base FPN model. However, there are still a few challenging examples which prove to be difficult for the proposed framework. These are analysed in the following section.

4.3 Analysis of challenging samples

A few examples for which the proposed GEO-FPN model is challenged are shown below.

Figure 7a contains 7 objects in total, and 6 of which are detected by the FPN model. One object can not be detected in any of the five frames, which can be due to the overlap with one of the several star trails in the background.

In Figure 7b, all frames in the sequence are overexposed, and this leads to extremely low signal-to-noise ratio for 3 out of 4 objects.

In Figure 7c, all frames in the sequence are impacted by the blurring due to the atmospheric effects, and this reduces the amplitude of the signal.

Figure 7a: Sample with overlaps with background stars

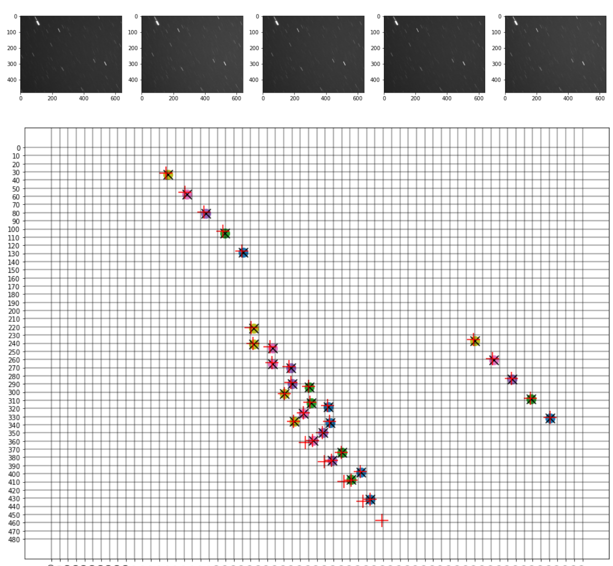

Figure 7b: Sample with overexposed frames

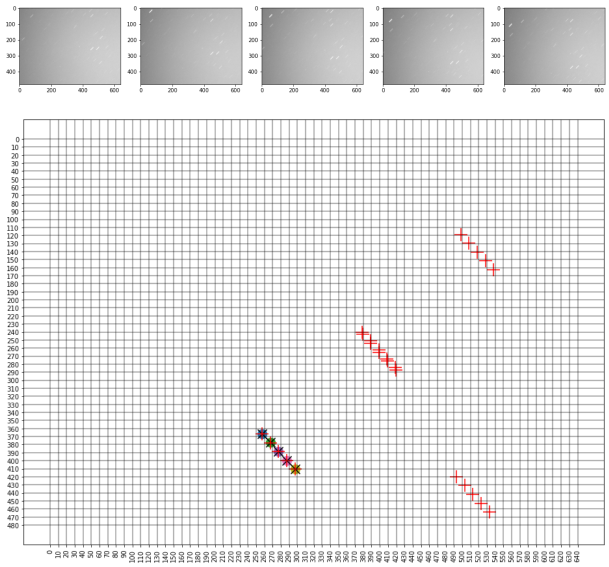

Figure 7c: Sample with blurred frames

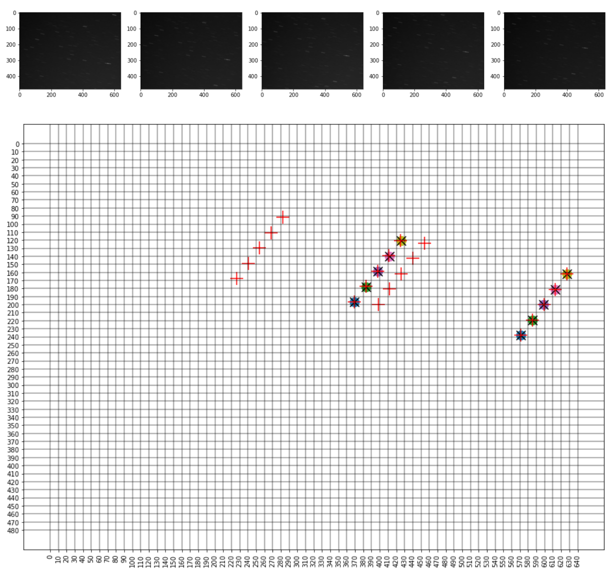

Figure 7: Challenging examples in the dataset

5 CONCLUSION AND FUTURE WORK

The proliferation of resident space objects in the last decades requires the automation of space surveillance operations to keep pace with the increasing number of trackable space objects. The proposed work shows that it is feasible to use advanced Computer Vision algorithms that can be trained end-to-end for space object detection in the telescope images. With an overall accuracy of 92%, our model is robust to many problematic effects such as atmospheric conditions, sensor defects and star occultations.

For future work, denoising labels, increasing the size of the dataset, and augmenting the dataset using simulated data are data-centric improvements that the authors will investigate for the problem. In addition, the dataset is not balanced regarding over-exposed images and crowded scenes, and the authors will incorporate data similar to the minority classes to balance the dataset.

6 ACKNOWLEDGEMENTS

We would like to thank ESA Advanced Concepts Team and University of Adelaide for hosting the SpotGEO challenge and providing the dataset that enabled us to introduce GEO-FPN in this paper.

7 REFERENCES

1 Holzinger, M. J. and Jah, M. K., 2018. Challenges and Potential in Space Domain Awareness. *Journal of Guidance, Control, and Dynamics*, *41*(1), pp.15-18.

2 ESA, Space debris by the numbers. 2021 https://www.esa.int/Safety_Security/Space_Debris/Space_debris_by_the_numbers.

3 Schildknecht, T., Musci, R., Flury, W., Kuusela, J., de Leon, J. and Dominguez Palmero, L., 2005, August. Optical observations of space debris in high-altitude orbits. In *4th European Conference on Space Debris* (Vol. 587, p. 113).

4 Seitzer, P., Smith, R., Africano, J., Jorgensen, K., Stansbery, E. and Monet, D., 2004. MODEST observations of space debris at geosynchronous orbit. *Advances in Space Research*, *34*(5), pp.1139-1142.

5 Blasch, E., Shen, D., Jia, B., Wang, Z., Chen, G., Chen, Y. and Pham, K., 2019, July. Autonomy in use for space situational awareness. In *Sensors and Systems for Space Applications XII* (Vol. 11017, p. 1101707). International Society for Optics and Photonics.

6 Yanagisawa, T., Nakajima, A., Kimura, T., Isobe, T., Futami, H. and Suzuki, M., 2002. Detection of small GEO debris by use of the stacking method.

Transactions of the Japan Society for Aeronautical and Space Sciences, *44*(146), pp.190-199.

7 Yanagisawa, T., Kurosaki, H., Banno, H., Kitazawa, Y., Uetsuhara, M. and Hanada, T., 2012, September. Comparison between four detection algorithms for GEO objects. In *Proceedings of the Advanced Maui Optical and Space Surveillance Technologies Conference* (Vol. 1114, p. 9197).

8 Yanagisawa, T., Kurosaki, H. and Nakajima, A., 2009, September. Activities of JAXA's innovative technology center on space debris observation. In *Advanced Maui Optical and Space Surveillance Technologies Conference, Poster presentations* (Vol. 23, p. 40).

9 Nakajima, A., 2000. Space Debris Observation by Ground-Based Optical Telescope. In *Proc. 22nd Int. Symp. Space Technology and Science, 2000*.

10 Šára, R., Matoušek, M. and Franc, V., 2013. RANSACing optical image sequences for GEO and near-GEO Objects. In *Proceedings of the Advanced Maui Optical and Space Surveillance Technologies Conference*.

11 Do, H.N., Chin, T.J., Moretti, N., Jah, M.K. and Tetlow, M., 2019. Robust foreground segmentation and image registration for optical detection of GEO objects. *Advances in Space Research*, *64*(3), pp.733-746.

12 Liu, D., Chen, B., Chin, T.J. and Rutten, M.G., 2020. Topological Sweep for Multi-Target Detection of Geostationary Space Objects. *IEEE Transactions on Signal Processing*, *68*, pp.5166-5177.

13 ESA and University of Adelaide, SpotGEO Challenge Hosted on Kelvins Platform. 2020 https://kelvins.esa.int/spot-the-geo-satellites/.

14 Lin, T.Y., Dollár, P., Girshick, R., He, K., Hariharan, B. and Belongie, S., 2017. Feature pyramid networks for object detection. In *Proceedings of the IEEE conference on computer vision and pattern recognition* (pp. 2117-2125).

15 Tan, M. and Le, Q., 2019, May. Efficientnet: Rethinking model scaling for convolutional neural networks. In *International Conference on Machine Learning* (pp. 6105-6114). PMLR.